

## Scaling of the velocity power spectra in turbulent thermal convection

Xiao-Dong Shang and Ke-Qing Xia\*

*Department of Physics, The Chinese University of Hong Kong, Shatin, Hong Kong, China*

(Received 3 May 2001; published 19 November 2001)

We report measurements of the local velocity in a convection cell filled with water. In the buoyancy subrange (the scales between the Bolgiano scale  $f_B$  and the integral scale  $f_o$ ), two scaling regions of the velocity frequency power spectra, separated by the peak frequency  $f_p$  of the dissipation spectra, are found. For  $f_p < f < f_B$ , we observe a power law with the Bolgiano-Obukhov scaling exponent  $-11/5$ . For  $f_o < f < f_p$ , an unexpected scaling with an exponent  $-1.35$  is observed. We also found that the velocity power spectra are universal functions with respect to the characteristic scales  $f_p$  and  $f_B$ .

DOI: 10.1103/PhysRevE.64.065301

PACS number(s): 47.27.Te, 44.25.+f, 05.40.-a, 94.10.Lf

Turbulent thermal convection continues to attract considerable interests as a model system for turbulence studies. An important issue in the study of turbulent convection is to determine the relevant dynamics that drive turbulent energy cascade at different length scales, which is manifested as different scaling laws of the energy spectrum for different ranges of the wave number. Bolgiano and Obukhov (BO) have long proposed, based on dimensional arguments, that for stably stratified convection two different dynamics control the cascade of turbulent energy within the usual inertial range. Above the Bolgiano length  $l_B$  is the so-called buoyancy subrange in which buoyancy is the dominant force, and one has the BO scaling where the energy spectrum decays with a power law  $k^{-11/5}$ ; below  $l_B$  inertia becomes the driving force and one observes the Kolmogorov-Obukhov (KO) scaling with  $k^{-5/3}$  [1]. Subsequently, BO scaling has been more rigorously shown to hold for unstably stratified convection as well [2–4], to which the Rayleigh-Bénard configuration belongs. Furthermore, it is revealed that BO scaling corresponds to an energy cascade with a scale-independent entropy flux, as opposed to a constant energy flux for KO scaling [3].

While the statistics and scaling properties of the temperature field appears to be well studied experimentally [5,6], corresponding studies in the velocity field remain scarce. The first measurement of the scaling properties of the velocity field was done in water convection by a homodyne spectroscopy technique, where a first-order velocity structure function  $\langle \delta v(\ell) \rangle$ , integrated over the distance  $\ell$ , was measured and BO scaling was observed [7]. More recently, velocity spectra with an exponent close to the predicted BO value was also observed in a laser Doppler velocimetry (LDV) measurement in gas convection near the gas-liquid critical point, in which critical density fluctuations were used as scatterers [8]. Thus, although BO scaling has been observed in the velocity spectra to various degrees, more direct and detailed study of the velocity spectra are clearly needed.

In this Rapid Communication, we report results from local velocity measurements in a Rayleigh-Bénard convection cell filled with water. The cell is a cylinder of inner diameter 19 cm with a height  $L=19.6$  cm, and its upper and lower

plates are made of copper with gold-plated surface. The temperature of the upper plate is regulated by passing cold water through a chamber fitted on its top. To ensure temperature uniformity of the top plate, the cooling chamber is fitted with two inlets and two outlets and with stirring blades driven by the incoming water jets. The lower plate is heated at a constant rate with an imbedded film heater. The temperature difference  $\Delta T$  between the two plates is monitored by four thermistors imbedded inside the plates. The measured relative temperature difference between the two thermistors in the same plate is less than 1% for both plates at all Rayleigh numbers (Ra), the rms temperature fluctuation is less than  $0.01^\circ\text{C}$  for the top plate and  $0.04^\circ\text{C}$  for the bottom. The vertical component of the velocity is measured for seven Rayleigh numbers, which are listed in Table I with the corresponding values of  $\Delta T$  and Prandtl numbers (Pr). For  $\text{Pr}=3.07$  the fluid's mean temperature is  $\sim 59^\circ\text{C}$ , and thus a Pyrex glass cylinder is used as the sidewall instead of the Plexiglas one as the case for other points. Qiu *et al.* have recently shown that, apart from regions near the top and bottom thermal boundary layers, LDV is capable of measuring local velocity in turbulent convection in water [9]. In our experiment, a commercial LDV (Dantec Ltd.) is used to measure the local velocity near the vertical sidewall of the convection cell. The size of the LDV measuring volume is about  $75\ \mu\text{m}$  and the fluid is seeded with neutrally buoyant  $2\text{-}\mu\text{m}$  diameter latex spheres as scatterers.

TABLE I. Rayleigh, Prandtl, and Reynolds numbers, and the local mean and the rms velocities of the seven spectra. Also listed are the corresponding temperature difference across the convection cell.

$\Delta T$ ( $^\circ\text{C}$ )	Ra	Pr	Re	$\bar{v}$ (mm/s)	$v_{rms}$ (mm/s)
1.26	$1.2 \times 10^8$	6.98	758	1.71	1.47
2.92	$2.9 \times 10^8$	6.97	1138	1.94	1.61
4.57	$4.8 \times 10^8$	6.80	1344	2.63	2.09
8.44	$9.9 \times 10^8$	6.50	1934	4.73	3.22
16.37	$2.4 \times 10^9$	5.91	3036	7.06	4.25
27.74	$7.3 \times 10^9$	4.30	6362	11.68	6.52
54.40	$2.3 \times 10^{10}$	3.07	13941	20.35	10.84

\*Corresponding author. Email address: kxia@phy.cuhk.edu.hk

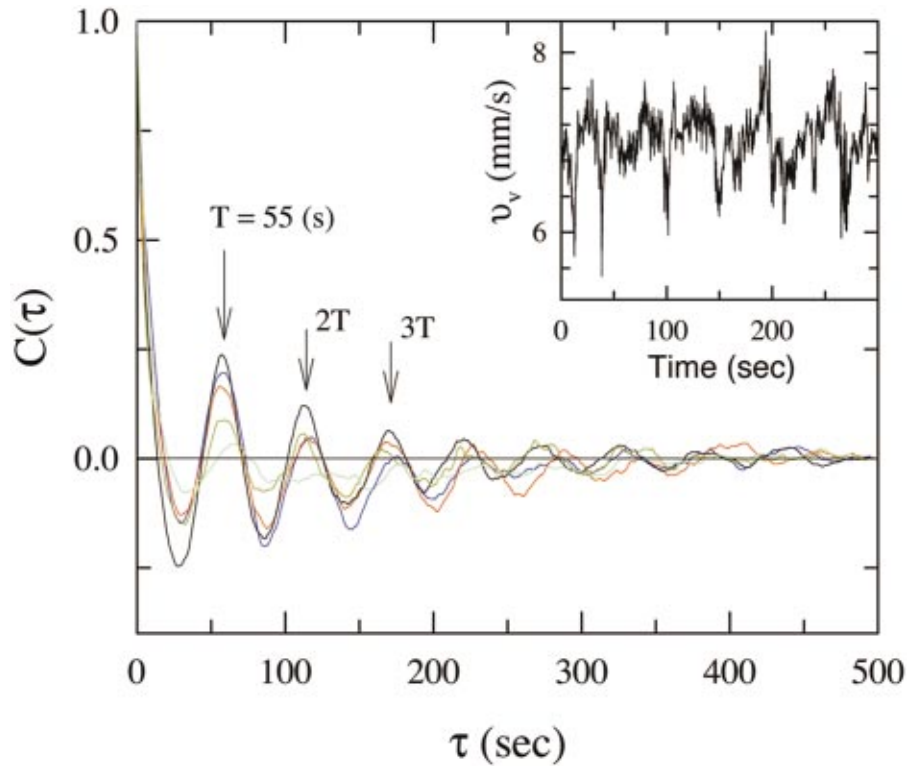


FIG. 1. (Color) Autocorrelation function  $C(\tau)$  of the vertical velocity measured at  $Ra=2.4 \times 10^9$  and at respective distances  $x = 0.5$  cm (red), 1.3 (blue), 2.7 (black), 4.0 (dark yellow), and 10.0 (green) from the sidewall. Inset: A segment of the velocity time series for  $x=2.7$  and for the same  $Ra$ .

We examine first the measured autocorrelation function of velocity fluctuations  $C(\tau) = \langle \delta v(t+\tau) \delta v(t) \rangle / \langle (\delta v)^2 \rangle$ , where  $\delta v = v - \bar{v}$ . Figure 1 plots several  $C(\tau)$ s as a function of the lag time  $\tau$  for  $Ra=2.4 \times 10^9$ , taken at respective distances  $x=0.5$  cm (red), 1.3 (blue), 2.7 (black), 4.0 (dark yellow), and 10.0 (green) from the sidewall, all at mid-height of the cell and within the rotational plane of the large-scale circulation (the arrows indicate the peaks for  $x=2.7$ ). The inset shows a 300-sec segment of the velocity time series for the position  $x=2.7$  cm. From the time series, we see that the velocity has large periodic excursions ( $\sim 50$  s), both positive and negative, from the mean, which corresponds well to the period  $T$  given by  $C(\tau)$ . These excursions represent the sudden accelerations and decelerations, or oscillations (but not directional reversals) of the large scale flow, and that  $C(\tau)$  remains correlated for many periods implies this periodic fluctuation of the mean flow is highly coherent. The existence of the large scale circulation in turbulent convection has long been observed by flow visualization and other methods, the correlation function now provides a more quantitative measure of its coherence. The mean velocity profiles we obtained are similar to that reported by Qiu *et al.* [9], for example, the mean velocity  $\bar{v}$  becomes linearly dependent on the distance when it is less than  $v_{rms}$ . For the present  $Ra$ ,  $x=0.5$  is close to the viscous boundary layer, the positions  $x=1.3, 2.7$ , and 4.0 are in the so-called mixing zone [9], where  $\bar{v} > v_{rms}$  and  $x=10.0$  is near the cell center. Note that  $C(\tau)$  for  $x=10.0$  cm (green curve) becomes rather noisy after the first peak. This is probably due to the zero mean

velocity in this position, which results in low data rate and reduced signal to noise ratio. Nevertheless, it is seen that even at this position the signature of an oscillatory flow can still be detected. All power spectra presented below are measured at positions about 2.7 cm from the sidewall and at mid-height.

It is seen from Fig. 1 that the frequency of coherent velocity oscillation  $f_o = T^{-1}$  [first peak of  $C(\tau)$ ] of the large-scale flow is approximately position-independent. We thus take this characteristic frequency  $f_o$  as the scale of energy injection (or the integral scale) in the frequency domain. We also define a Reynolds number  $Re = (4Lf_o)L/\nu$  based on  $f_o$ . The values of  $Re$  together with the mean and rms values of the local velocity where the power spectra are taken are listed in Table I. In turbulence studies, theoretical results are usually presented in the wave-number domain, while experimental data are in the frequency domain. To make a comparison, one usually needs to invoke Taylor's frozen-flow hypothesis, which in general, requires the mean flow is much larger than the rms velocity. In turbulent convection, the mean velocity is generally not much larger than the rms value in most part of the cell (as can be seen from Table I), and is zero in the cell center where many measurements have been made [5,7]. Although, a coincidence between experimentally measured wave-number spectra and frequency spectra of the temperature in thermal convection was found [6], the use of Taylor's assumption should nonetheless be handled with caution. In below, we present all results in the frequency domain, but bear in mind that it is the wave-number spectrum from theory that we are comparing with.

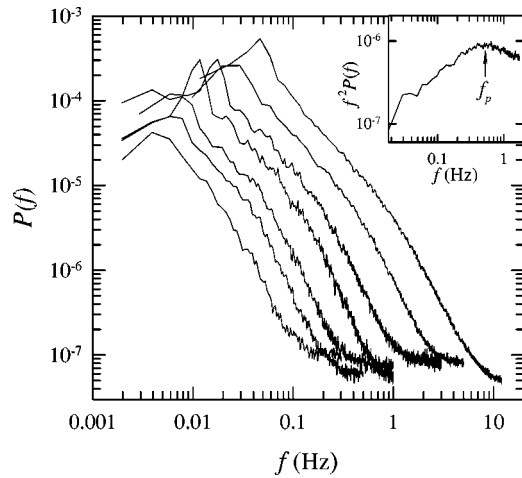


FIG. 2. Frequency power spectra of the measured vertical velocity, with  $Ra$  increasing from left to right. Inset: Dissipation spectrum for  $Ra=7.3 \times 10^9$ .

The acquisition time of all our velocity data is 7 hours with the mean data rate ranging from 14 to 61 Hz, the obtained velocity records thus contain from  $3.5 \times 10^5$  to  $1 \times 10^6$  data points. With the acquired velocity time series, we obtain the frequency power spectra using a fast Fourier transform program provided by Dantec. In calculating the spectrum, the program uses a resampling technique [“sample and hold” (S and H)] to interpolate the irregularly spaced time series that is inherent to the LDV technique. The S and H method has been shown to produce accurate spectra for frequencies up to  $n/2\pi$ , where  $n$  is the mean data rate [10] and all our data satisfy this criterion. As a check, we also did a linear interpolation to convert the velocity data into equal-time-spaced records and then calculated the spectra using the software MATLAB, and find good agreement between the two methods.

Figure 2 shows the velocity frequency power spectra  $P(f)$  for the seven  $Ra$  numbers. The peak near the low-frequency end indicates the oscillation frequency  $f_o = T^{-1}$  of the mean flow, as already obtained from the correlation function. But with the correlation function, we can determine the oscillation time more accurately than from the power spectra (due to the latter’s uneven spectra point distribution in the log scale). We find that velocity power spectra measured in other positions in the mixing zone are similar to those in Fig. 2. The peak wave number  $k_p$  of the energy dissipation spectra  $k^2 E(k)$  has been shown to be the characteristic scale for the collapsing of the kinetic-energy spectra for Navier-Stokes turbulence [11], and the same feature is also observed recently for temperature frequency power spectra [12]. The inset of Fig. 2 shows an example of the velocity dissipation spectra  $f^2 P(f)$ , where the peak frequency  $f_p$  at which dissipation reaches maximum is indicated (the exact values of  $f_p$  are determined through a six-order polynomial fit). We show in Fig. 3 the scaled spectra  $P(f)/P(f_p)$  versus the scaled frequency  $f/f_p$  in a log-log plot. It is seen that  $f_p$  is indeed the characteristic frequency with respect to which velocity power spectra for different values of  $Ra$  have a universal form. Figure 3 also reveals the existence of two power-law regions in the spectra roughly separated by  $f_p$ . In the figure,

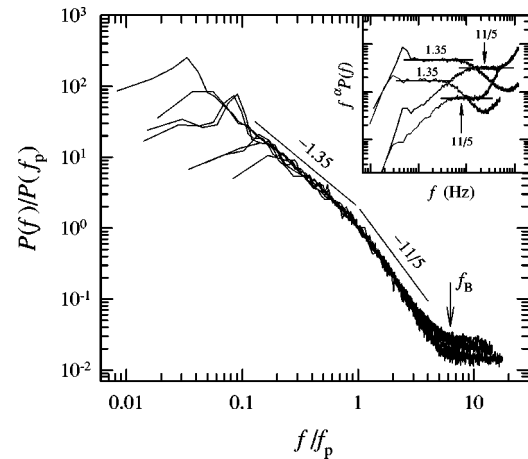


FIG. 3. Scaled velocity spectra for the ones shown in Fig. 2. Inset: Compensated spectra  $f^\alpha P(f)$  for  $Ra=7.3 \times 10^9$  (light lines) and  $2.3 \times 10^{10}$  (dark lines) and for  $\alpha=1.35$  and  $11/5$ , respectively.

$f_B$  indicates the frequency corresponding to the Bolgiano length (see below). A best fit to the “low-frequency” scaling region yields an exponent of  $-1.35$ . The inset of Fig. 3 shows compensated spectra  $f^\alpha P(f)$  versus  $f$  for  $\alpha=1.35$  and  $11/5$ , and for two values of  $Ra$ , respectively. Here, the theoretically predicted exponent  $-11/5$  for the BO scaling of the velocity spectra is used. The highly sensitive compensated plot clearly shows the existence of two power-law regions with very different exponents. The two solid lines in the main figure have slopes exactly as indicated. Thus, starting from the integral scale  $f_o$ , the velocity spectra decays as a power law with an exponent of  $-1.35$  to a scale around  $f_p$  and then continue to decay with the much steeper BO exponent  $-11/5$  down to the Bolgiano scale  $f_B$ .

In Fig. 4 we plot the  $Ra$  dependence of the few relevant frequency scales,  $f_o$  (up triangles) obtained from the auto-correlation function and  $f_p$  (solid circles) from the dissipation spectra. The solid lines are simple power-law fits:  $f_o = 2.3 \times 10^{-6} Ra^{0.42 \pm 0.01}$  and  $f_p = 2.58 \times 10^{-8} Ra^{0.74 \pm 0.02}$ . The open circles in Fig. 4 are the calculated “Bolgiano frequency”  $f_B = \bar{v}/l_B$ , where  $\bar{v}$  is the local mean velocity and  $l_B = LNu^{1/2}/(RaPr)^{1/4}$  is the theoretically predicted Bolgiano

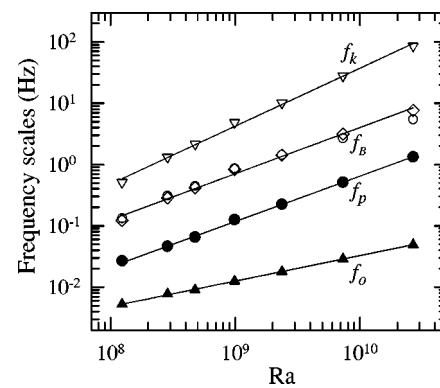


FIG. 4. Rayleigh number dependencies of the characteristic frequency scales  $f_o$ ,  $f_p$ ,  $f_B$  (open circles),  $f_B(5.9/Pr)^{0.49}$  (diamonds), and  $f_k$ . See text for the power-law fits.

length [6] for which the experimental values of Nu, Ra, and Pr are substituted. Also shown is the similarly-obtained dissipation scale  $f_k$  (down triangles), corresponding to the Kolmogorov length  $\eta_k = LPr^{-1/2}/(RaNu)^{1/4}$  [6] and the solid line is a power-law fit  $f_k = 1.38 \times 10^{-8} Ra^{0.94 \pm 0.02}$ . Notice that  $f_B$  shown in the figure appears to curve slightly. From Table I we see the Prandtl number varied by a factor of two, thus  $f_B$  is plotted against Ra without holding Pr as a constant. Combining the Pr dependence of  $\bar{v}$  and that of  $l_B$ , we obtain  $f_B \sim Pr^{0.49}$  [13]. To account for this Pr variation, we multiply  $f_B$  by  $(5.9/Pr)^{0.49}$  and the results are shown as diamonds in Fig. 4. It is seen that, except for the lowest point, normalizing data to a fixed Pr(=5.9) brings most points closer to a straight line. The value 5.9 is chosen because it is in the middle of the range (third point from right), which results in the least change in the overall magnitude of  $f_B$  ( $f_k$ , on the other hand, has a much weaker Pr dependence than that of  $f_B$ , so is less scattered). Figure 4 shows that  $f_B$  and  $f_p$  have essentially the same Ra dependence, and a power-law fit (top solid line) to the diamonds produces an exponent of  $0.75 \pm 0.02$  for  $f_B$ . By fixing this exponent to 0.74 we obtain  $f_B \approx 6f_p$ . This is indicated in Fig. 3 where we see that  $f_B$  is essentially the frequency at which the velocity spectra  $P(f)$  intersects the noise floor and thus is the cutoff frequency of turbulent kinetic-energy excitation. This implies that there is no further cascade of energy beyond the so-called buoyancy subrange for the present range of Ra and Pr, and this happens at frequencies much smaller than the dissipation scale  $f_k$ . Note that the constant ratio between  $f_B$  and  $f_p$  implies the spectra can also be scaled with respect to  $f_B$ , which is indeed the case. It has been theoretically predicted that the range for BO scaling increases with increasing Ra [2]. But due to the existence of the new  $-1.35$  scaling, it is seen from Fig. 4 (and also Fig. 3) that although the overall scaling range (the gap between  $f_B$  and  $f_o$ ) is increased with increasing Ra, this increase goes almost entirely to the new scaling region (the gap between  $f_p$  and  $f_o$ ) and the range for the Bolgiano scaling increases very little. Because the ‘‘original’’ buoyancy subrange now contains two scaling ranges, the range of the BO scaling is shortened, which is about half a decade as seen from Fig. 3.

In most studies of temperature fluctuations in turbulent convection, only BO scaling was observed [5,6] and there appears to be mixed results for the existence of K41-type scaling [14]. Recently, there is evidence that different scalings may exist in different regions of the cell [12]. In any case, no power-law decay was observed for scales larger than  $l_B$  other than the BO scaling. While it is not clear to us why only BO scaling was observed in the earlier studies of velocity spectra, we note that the measured velocity structure function in Ref. [7] was integrated along the slit width over where velocity difference was taken; and for the work reported in Ref. [8], the authors noted that the high level of white noise significantly limits the dynamic range of their spectra. Recently, Qiu *et al.* observed evidence that the rising and falling plumes along the sidewall of the cell may act coherently to provide a driving mechanism for the large-scale mean flow [9]. Indeed, by considering the possibility that thermal plumes can impart kinetic energy to the velocity field both directly and via buoyancy, Grossmann and Lohse have obtained a velocity spectrum that shows a decay slower than either BO or KO scaling [15]. But this plume-driven regime was predicted to occur at length scales smaller than the Bolgiano length, i.e., following the buoyancy-driven range, which is opposite to the findings here. Clearly, further investigations, both theoretical and experimental, are needed to understand the new scaling.

In summary, we have made local velocity measurements in a water convection cell for over two decades of Rayleigh numbers. In the buoyancy subrange (the scales between  $f_B$  and  $f_o$ ), two scaling regions separated by the peak frequency  $f_p$  of the dissipation spectra are observed in the velocity frequency power spectra. For  $f_p < f < f_B$ , we observe a power law with an exponent that is in excellent agreement with the predicted Bolgiano-Obukhov value of  $-11/5$ . For  $f_o < f < f_p$ , an unexpected scaling with an exponent of  $-1.35$  is observed. We also found that the velocity spectra can be scaled to collapse on a single curve with respect to  $f_p$  as well as  $f_B$ .

We gratefully acknowledge support of this work by the Research Grants Council of Hong Kong SAR under Grant No. CUHK 4224/99P.

- 
- [1] R. Bolgiano, J. Geophys. Res. **64**, 2226 (1959); A.M. Obukhov, Dokl. Akad. Nauk. SSSR **125**, 1246 (1959). [Sov. Phys. Dokl. **4**, 61 (1959)].
- [2] I. Procaccia, and R. Zeitak, Phys. Rev. Lett. **62**, 2128 (1989).
- [3] V.S. L'vov, Phys. Rev. Lett. **67**, 687 (1991).
- [4] V. Yakhot, Phys. Rev. Lett. **69**, 769 (1992).
- [5] X.-Z. Wu *et al.*, Phys. Rev. Lett. **64**, 2140 (1990).
- [6] F. Chillá *et al.*, Nuovo Cimento D **15**, 1229 (1993).
- [7] P. Tong and Y. Shen, Phys. Rev. Lett. **69**, 2066 (1992).
- [8] S. Ashkenazi and V. Steinberg, Phys. Rev. Lett. **83**, 4760 (1999).
- [9] X.-L. Qiu *et al.*, Phys. Rev. E **61**, R6075 (2000).
- [10] R.J. Adrian and C.S. Yao, Exp. Fluids **5**, 17 (1987).
- [11] Z.-S. She and E. Jackson, Phys. Fluids A **5**, 1526 (1993).
- [12] S.-Q. Zhou and K.-Q. Xia, Phys. Rev. Lett. **87**, 064501 (2001).
- [13] In a separate measurement over a wide range of Pr, we find  $Re = 1.1Ra^{0.43}Pr^{-0.76}$  (unpublished). As the change in Pr for our data is mostly due to the kinematic viscosity  $\nu$  (it more than doubled), we treat the thermal diffusivity  $\kappa$  (change  $\sim 10\%$ ) as a constant. This gives  $\bar{v} \sim Pr^{0.24}$ . Ignoring a possibly weak Pr dependence of Nu, we have  $l_B \sim Pr^{-0.25}$ , which leads to  $f_B \sim Pr^{0.49}$ .
- [14] J.A. Glazier *et al.*, Nature (London) **398**, 307 (1999); J.J. Niemela *et al.*, *ibid.* **404**, 837 (2000).
- [15] S. Grossmann and D. Lohse, Phys. Rev. A **46**, 903 (1992).